arXiv:hep-ex/0406064v1 23 Jun 2004

Latest Results from NA48 and NA48/1

M. W. SLATER

Department of Physics, High Energy Physics, Cavendish Laboratory,
Madingley Road, Cambridge CB3 0HE, England

The first observations of the rare decays $K_S \to \pi^0 e^+ e^-$ and $K_S \to \pi^0 \mu^+ \mu^-$ have been made by the NA48/1 collaboration at the CERN SPS accelerator. From high intensity K_S data collected during the 2002 run, clean signals of 7 $K_S \to \pi^0 e^+ e^-$ events and 6 $K_S \to \pi^0 \mu^+ \mu^-$ events were observed, giving branching ratio measurements of $BR(K_S \to \pi^0 e^+ e^-) = 5.8^{+2.9}_{-2.4} \times 10^{-9}$ and $BR(K_S \to \pi^0 \mu^+ \mu^-) = 2.9^{+1.5}_{-1.2} \times 10^{-9}$. These results constrain the indirect CP violating component of the corresponding K_L decays. Other recent results from NA48 are also presented.

1 Introduction

The NA48 experiment was originally designed to measure the CP violation parameter $\text{Re}(\frac{\epsilon'}{\epsilon})$ via a high statistics comparison of $K_S \to \pi\pi$ and $K_L \to \pi\pi$ decays. A beamline consisting of simultaneous K_S and K_L beams was used, with a tagging system allowing discrimination between the two types of kaon. Rare K_L decay and precision measurements could be carried out in parallel. In 2002, for the NA48/1 phase of the experiment, the K_L beam was removed and the proton intensity on the K_S target was increased by a factor ~ 1000, allowing very rare K_S and hyperon decay searches to be pursued.

The kaon beams were produced using 400 GeV/c protons provided by the Super Proton Synchrotron (SPS) at CERN, incident on two separate beryllium targets. The NA48 detector consisted of the following principal sub-detectors: a magnetic spectrometer consisting of 4 drift chambers separated by a dipole magnet, a high resolution liquid krypton electromagnetic calorimeter, an iron scintillator hadronic calorimeter and a muon system consisting of 3 planes of scintillator shielded by 80cm thick iron walls.[1]
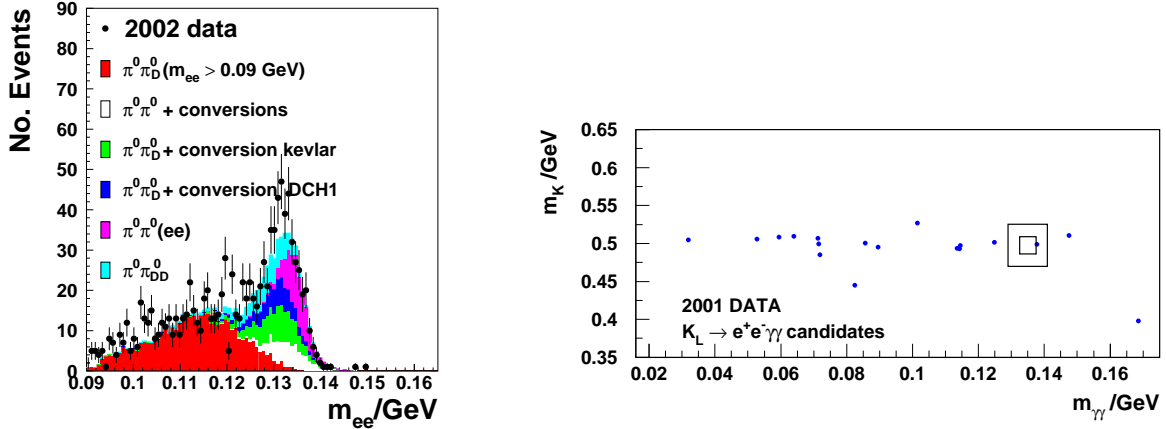
Figure 1: (a) m_{ee} distribution of the Dalitz decay and conversion background. Reasonable agreement between data (points) and Monte Carlo (curves) can be seen. (b) 2001 data showing the distribution of the $K_L \to ee\gamma\gamma$ background across the signal region.

2 Physics Motivation for $K_S \to \pi^0 l^+ l^-$ Searches

The decay mode $K_L \to \pi^0 \nu \bar{\nu}$ is direct CP violating and can be used to determine the parameter η in the Wolfenstein parameterisation of the CKM matrix. This channel is theoretically very clean but is experimentally challenging due to the missing energy from the neutrinos. A second possibility to measure η is from the decay $K_L \to \pi^0 l^+ l^-$. This decay is easier to measure experimentally as all the decay products are detectable, but is more complicated theoretically as it has contributions from CP conserving and both direct and indirect CP violating components, which also interfere. The CP conserving component can be predicted from a measurement of $K_L \to \pi^0 \gamma\gamma$ while the indirect CP violating component can be predicted from a measurement of $K_S \to \pi^0 l^+ l^-$. Any measurement of $BR(K_L \to \pi^0 l^+ l^-)$, and consequently, η, requires the measurement of $BR(K_S \to \pi^0 l^+ l^-)$ to disentangle the direct from the indirect CP violating components.

3 Analysis Strategy for $K_S \to \pi^0 e^+ e^-$ and $K_S \to \pi^0 \mu^+ \mu^-$

Both $K_S \to \pi^0 e^+ e^-$ and $K_S \to \pi^0 \mu^+ \mu^-$ were predicted to have very small branching ratios, ($\sim 10^{-9}$) and so, even with a flux of $\sim 3 \times 10^{10}$ K_S decays, only a handful of events were expected from either channel. Therefore, to avoid biasing the results, a blind analysis procedure was employed. A $2.5\sigma_{m_K} \times 2.5\sigma_{\pi^0}$ signal region and a $6.0\sigma_{m_K} \times 6.0\sigma_{\pi^0}$ control region were defined. Both regions were kept masked during the background studies. Only after the background contributions to the signal had been estimated and the cuts fixed was the control region unmasked. Final selection changes could then be made if required before the signal region was unmasked.

4 $K_S \to \pi^0 e^+ e^-$

4.1 Signal Selection

$K_S \to \pi^0 e^+ e^-$ candidates were selected with $40 < E_K < 240 \mathrm{GeV}$ and within 2.5 K_S lifetimes of the end of the final collimator. Two oppositely charged tracks, with $E/p > 0.95$ and forming a good vertex, were required, as well as two clusters in the calorimeter that were not associated to tracks.
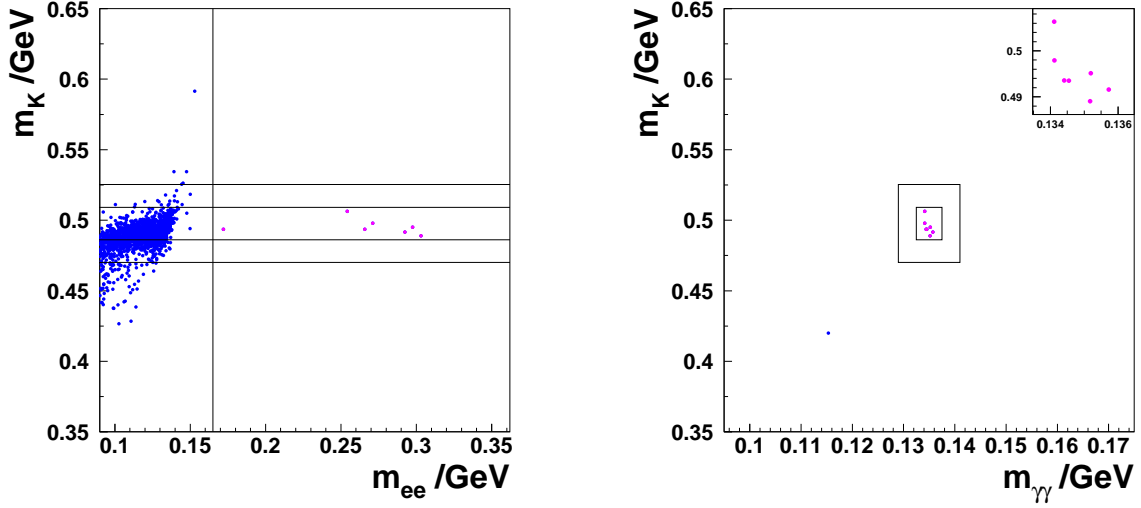
Figure 2: The (a) $m_{\gamma\gamma}$ vs. m_{ee} and (b) $m_{\gamma\gamma}$ vs. m_K mass planes showing $K_S \to \pi^0 e^+ e^-$ candidate events. The large background from dalitz decays and photon conversions can be seen at low m_{ee}

4.2   Background

Backgrounds for the $K_S \to \pi^0 e^+ e^-$ decay were divided into two categories: physical background (arising from a single kaon decay), and accidental background (arising from two separate, over-lapping kaon decays). Three significant sources of physical background were identified. The first came from Dalitz decays ($\pi^0 \to ee\gamma$) and photon conversion in the various parts of the detector. These backgrounds were studied extensively using Monte Carlo simulation (see fig. 1a). Reason-able agreement with data was found in the m_{ee} distribution around the π^0 mass. A conservative cut of $m_{ee} > 0.165\,\text{GeV}/c^2$ was applied to remove this background, with a corresponding 48% loss in acceptance.

The second significant physical background was identified as $K_L \to ee\gamma\gamma$. This background spread across the $m_{\gamma\gamma}$ signal region as can be seen in fig. 1b. Using K_L data taken in 2001, the background was estimated to be $0.08^{+0.03}_{-0.02}$ events.

The final physical background came from various hyperon decay channels. The beam contained a significant ($\sim 10^9$) flux of neutral hyperons and the channels $\Xi^0 \to \Lambda(p\pi^-)\pi^0$, $\Xi^0 \to \Lambda(pe^-\nu)\pi^0$ and $\Xi^0 \to \Sigma^+(p\pi^0)e^-\nu$ were identified as possible background sources. A cut on the momentum asymmetry of the decay products reduced these backgrounds to a negligible level.

The accidental background was dominated by overlapping fragments of two decays, e.g $(K_L \to \pi^\pm e^\mp \nu) + (K_S \to \pi^0 \pi^0)$. This background was suppressed by cutting on the spread of track and cluster times ($|\Delta t| < 3$ns). To estimate the remaining accidental background, the timing cuts were relaxed and the time sidebands investigated. No events were found in the out of time (3ns $< |\Delta t| < 50$ns) signal region. Therefore, an extrapolation was made from the out of time control region to the out of time signal region, taking into account the shape of the background from Monte Carlo simulation. A further time extrapolation could then be performed to get the final background estimate for the in time region ($|\Delta t| < 3$ns) of 0.069 events.

4.3   Result

The overall background estimate was $0.15^{+0.05}_{-0.04}$ events. The control region was unmasked and no events were found. No changes to the selection were needed before the signal region was
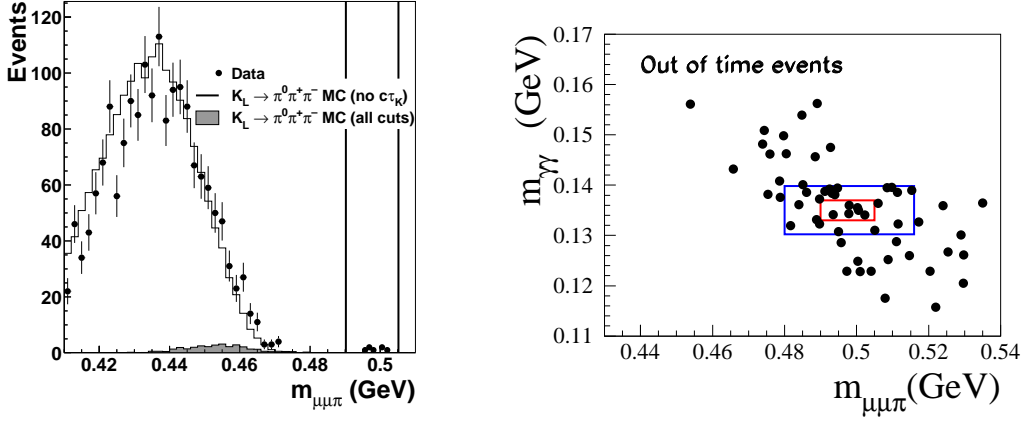
Figure 3: (a) The kaon mass region with the $K_L \to \pi^0 \pi^+ \pi^-$ background. Reasonable agreement between data and monte carlo (24 times the data) is shown. (b) Distribution of out of time events in the m_K vs. $m_{\gamma\gamma}$ plane.

unmasked. A signal of 7 events was found, giving the result: [2]

$$BR(K_S \to \pi^0 e^+ e^-) = (5.8^{+2.8}_{-2.3}(stat) \pm 0.8(syst)) \times 10^{-9} \tag{1}$$

where the systematic error is dominated by uncertainties arising from the extrapolation to the full m_{ee} region. The candidate events are shown in fig. 2.

5 $K_S \to \pi^0 \mu^+ \mu^-$

5.1   Signal Selection

$K_S \to \pi^0 \mu^+ \mu^-$ candidates were selected with $60 < E_K < 200 \text{GeV}$ and within 3 K_S lifetimes of the end of the final collimator. Two oppositely charged tracks were required that formed a good vertex, as well as two clusters in the calorimeter that were not associated to tracks. The tracks had to leave minimum energy in the calorimetry and have associated hits in the muon detector.

5.2   Background

As with $K_S \to \pi^0 e^+ e^-$, the backgrounds were divided into physical and accidental sources. Three dominant sources of physical background were identified. The first was $K_L \to \pi^0 \pi^+ \pi^-$ where the two charged pions had decayed in flight. This background was studied extensively in Monte Carlo, (see fig. 3a) and estimated to be ≤ 0.019 events. The second significant background was $K_L \to \mu^+ \mu^- \gamma\gamma$. This, again, was studied with Monte Carlo and estimated to contribute 0.04 ± 0.04 events to the overall background. The last physical background came from hyperon decays. As with $K_S \to \pi^0 e^+ e^-$, a cut on the momentum asymmetry of the decay products was used to reduce this background to a negligible level.

The accidental background was treated similarly to $K_S \to \pi^0 e^+ e^-$, by loosening the timing cuts and extrapolating into the in time ($|\Delta t| < 1.5$ns) region. 6 events were found in the out of time (-115ns $< \Delta t < 60$ns) signal region, leading to a background estimate of $0.18^{+0.18}_{-0.11}$ events. The distribution of these events in the mass plane is shown in fig. 3b.

5.3   Result

The overall background estimate was $0.22^{+0.19}_{-0.12}$ events. The control region was unmasked and no events were found. No changes to the selection were needed, the signal region was unmasked
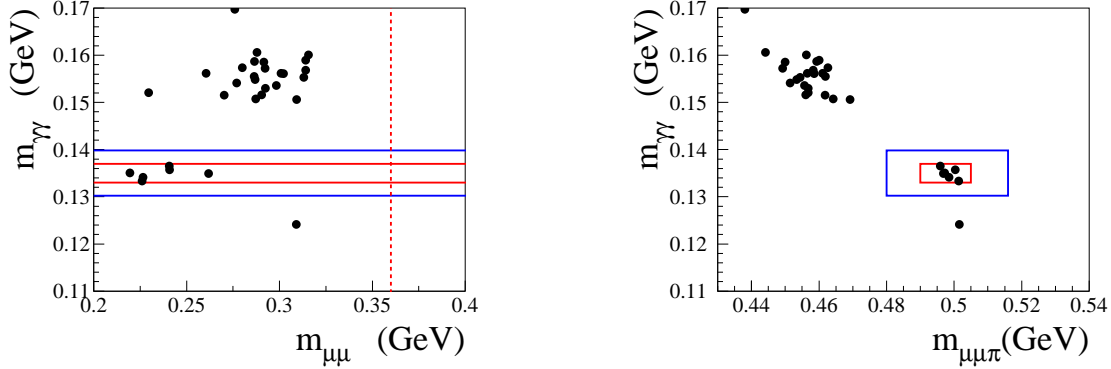
Figure 4: The (a) $m_{\gamma\gamma}$ vs. m_{ee} and (b) $m_{\gamma\gamma}$ vs. m_K mass planes showing $K_S \to \pi^0\mu^+\mu^-$ candidate events. The events at large $m_{\gamma\gamma}$ are consistent with $K_L \to \pi^0\pi^+\pi^-$ background and the single event at low $m_{\gamma\gamma}$ is consistent with accidental background

and 6 events were found. This led to the result:

$$BR(K_S \to \pi^0\mu^+\mu^-) = (2.9^{+1.5}_{-1.2}(stat) \pm 0.2(syst)) \times 10^{-9} \tag{2}$$

where the systematic error comes from uncertainties in the normalisation, obtained from $K_S \to \pi^+\pi^-$ decays. The candidate events are shown in fig. 4.

6 Interpretation of the $K_S \to \pi^0 l^+ l^-$ Measurements

The form factor for $K_S \to \pi^0 l^+ l^-$ decays can be described in Chiral Perturbation Theory by a first order polynomial:

$$W(z) \simeq G_F m_K^2(a_S + b_S z) \tag{3}$$

where $z = m_{ll}^2/m_K^2$. This leads to the following predictions for the $K_S \to \pi^0 l^+ l^-$ branching ratios:[3]

$$BR(K_S \to \pi^0 e^+ e^-) = [0.01 - 0.76a_S - 0.21b_S + 46.5a_S^2 + 12.9a_S b_S + 1.44b_S^2] \times 10^{-10} \tag{4}$$

$$BR(K_S \to \pi^0 \mu^+ \mu^-) = [0.07 - 4.52a_S - 1.50b_S + 98.7a_S^2 + 57.7a_S b_S + 8.95b_S^2] \times 10^{-11} \tag{5}$$

The Vector Meson Dominance (VMD) model predicts the ratio $b_S/a_S = 0.4$, allowing $|a_S|$ to be extracted for both channels:

$$BR(K_S \to \pi^0 e^+ e^-) \simeq 5.2 \times 10^{-9} a_S^2 \quad \Rightarrow |a_S|_{\pi^0 ee} = 1.06^{+0.26}_{-0.21} \pm 0.07 \tag{6}$$

$$BR(K_S \to \pi^0 \mu^+ \mu^-) \simeq 1.2 \times 10^{-9} a_S^2 \quad \Rightarrow |a_S|_{\pi^0 \mu\mu} = 1.55^{+0.38}_{-0.32} \pm 0.05 \tag{7}$$

These results for $|a_S|$ agree within errors.

By combining the ee and $\mu\mu$ results in a log-likelihood fit, a_S and b_S can be determined separately. As can be seen from fig. 5, the observed $K_S \to \pi^0 e^+ e^-$ and $K_S \to \pi^0 \mu^+ \mu^-$ rates are compatible with both each other and the VMD model.
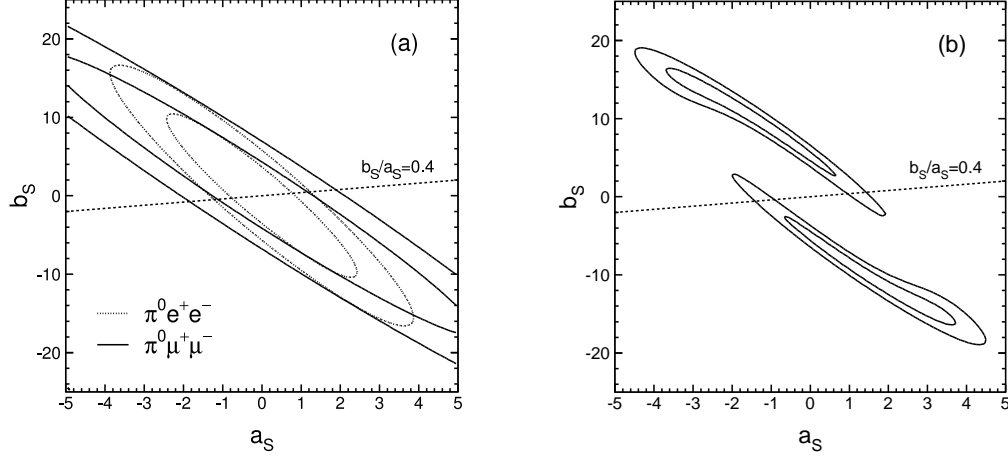
Figure 5: (a) Allowed regions of a_S and b_S determined from the observed number of $K_S \to \pi^0 e^+ e^-$ and $K_S \to \pi^0 \mu^+ \mu^-$ events separately. The region between the inner and outer elliptical contours is the allowed region at 68% CL. (b) Allowed regions of a_S and b_S for the $K_S \to \pi^0 e^+ e^-$ and $K_S \to \pi^0 \mu^+ \mu^-$ channels combined. The contours delimit the 1σ and 2σ allowed regions from the combined log-likelihood. The dashed straight line in both plots corresponds to $b_S = 0.4a_S$, as predicted by the VMD model.

7 Implications for $K_L \to \pi^0 l^+ l^-$

The CP violating component of the $K_L \to \pi^0 l^+ l^-$ branching ratio is given by:

$$BR(K_L \to \pi^0 l^+ l^-)_{CPV} \times 10^{12} = C_{IND} \pm C_{MIX} \left(\frac{\text{Im}(\lambda_t)}{10^{-4}} \right) \pm C_{DIR} \left(\frac{\text{Im}(\lambda_t)}{10^{-4}} \right)^2 \qquad (8)$$

where C_{DIR} is the direct CPV component, $C_{IND} \sim BR(K_S \to \pi^0 l^+ l^-)$ is the indirect CPV component, $C_{MIX} \sim \sqrt{BR(K_S \to \pi^0 l^+ l^-)}$ is the interference term and $\text{Im}(\lambda_t) = \text{Im}(V_{ts}^* V_{td})$.

The indirect CPV component and the interference term depend on the parameter $|a_S|$. Using the measured values of $|a_S|$ given above and taking [4] $\text{Im}(\lambda_t) = (1.36 \pm 0.12) \times 10^{-4}$ gives the following predictions for the central value of the $K_L \to \pi^0 l^+ l^-$ branching ratios:

$$BR(K_L \to \pi^0 e^+ e^-)_{CPV} \times 10^{12} \simeq 17_{\text{indirect}} \pm 9_{\text{interference}} + 5_{\text{direct}} \qquad (9)$$

$$BR(K_S \to \pi^0 \mu^+ \mu^-)_{CPV} \times 10^{12} \simeq 9_{\text{indirect}} \pm 3_{\text{interference}} + 1_{\text{direct}} \qquad (10)$$

where the sign ambiguity reflects the uncertainty in the sign of a_S.

8 $K_L \to \pi^\pm e^\mp \nu \gamma$

The most precise published measurement of $BR(K^0 \to \pi^\pm e^\mp \nu \gamma)$ comes from the KTeV collaboration[5]

$$BR(K^0 \to \pi^\pm e^\mp \nu \gamma)/BR(K^0 \to \pi^\pm e^\mp \nu) = (0.908 \pm 0.008^{+0.013}_{-0.012})\%, \qquad (11)$$

which is significantly below current theroretical predictions. This branching ratio has now been measured by NA48 using data from 1999. In order to reduce the uncertainties in the measurement due to radiative corrections, a model independent method was developed. The PHOTOS [6] package was used for the initial Monte Carlo generation. The Monte Carlo events were then weighted with the $\theta^*_{e\gamma}$ distribution, (the angle between the electron and the photon in the kaon rest frame). This gave good agreement between data and Monte Carlo for all distributions. The preliminary branching ratio measurement using this model independent method was found to be:

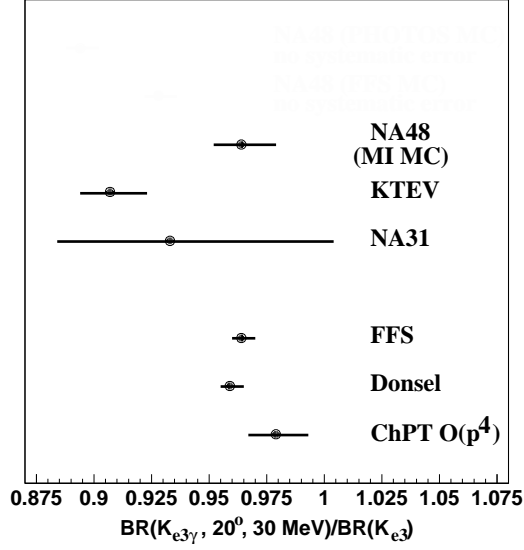$$BR(K^0 \to \pi^\pm e^\mp \nu \gamma)/BR(K^0 \to \pi^\pm e^\mp \nu) = (0.964 \pm 0.008^{+0.012}_{-0.011})\% \qquad (12)$$

Figure 6: The measured value of $BR(K^0 \to \pi^\pm e^\mp \nu \gamma)/BR(K^0 \to \pi^\pm e^\mp \nu)$ compared with the published result from the KTeV collaboration and theoretical predictions.

This is in good agreement with recent theoretical predictions, (Fearing, Fischbach and Smith (FFS)[7,8], Doncel[9] and Chiral Perturbation Theory calculations[10,11]), as can be seen from fig. 6. If the FFS method is used to apply the radiative corrections, as in the KTeV analysis, the result is found to be in agreement with the KTeV measurement.

9 $K_L \to \pi^0 \pi^\pm e^\mp \nu$

A high precision measurement of the branching ratio and form factors for the $K_L \to \pi^0 \pi^\pm e^\mp \nu$ decay was made using K_L data from 2001. This decay provides a good test of Chiral Perturbation Theory (CHPT) predictions for long distance meson interactions and the form factor measurements allow the determination of the CHPT parameter, L_3 .[12,13]

The main background to this decay was $K_L \to \pi^0 \pi^+ \pi^-$ where a pion was misidentified as an electron. To minimise this background, a neural network was used to distinguish between pions and electrons that took into account geometric characteristics of the showers and tracks. This reduced the background to 1.13%.

A signal of 5464 events was found with a background of 62 events. This gave a preliminary branching ratio measurement of:

$$BR(K_L \to \pi^0 \pi^\pm e^\mp \nu) = (5.21 \pm 0.07_{stat} \pm 0.09_{syst}) \times 10^{-5} \tag{13}$$

Assuming a V-A structure for the matrix element, the form factor parameters were then measured to be:

$$\bar{f}_s = 0.052 \pm 0.006_{stat} \pm 0.002_{syst}$$
$$\bar{f}_p = -0.051 \pm 0.011_{stat} \pm 0.005_{syst}$$
$$\lambda_g = 0.087 \pm 0.019_{stat} \pm 0.006_{syst}$$
$$\bar{h} = -0.32 \pm 0.12_{stat} \pm 0.07_{syst}$$

This led to the following value for L_3:

$$L_3 = (-4.1 \pm 0.2) \times 10^{-3} \tag{14}$$

10 $\Xi \to \Lambda\gamma$

Using data from a short test run from 1999 with a high intensity K_S beam alone, 730 $\Xi \to \Lambda\gamma$ events were found with a background of 58.2 ± 7.8 events. This led to a branching ratio measurement of:[14]

$$BR(\Xi \to \Lambda\gamma) = (1.16 \pm 0.05_{stat} \pm 0.06_{syst}) \times 10^{-3} \tag{15}$$

The statistics were large enough to enable a significant measurement of the decay asymmetry to be made:

$$\alpha(\Xi \to \Lambda\gamma) = -0.78 \pm 0.18_{stat} \pm 0.06_{syst} \tag{16}$$

This is the first evidence for a non-zero asymmetry in this decay mode. A much larger sample from the 2002 run is currently under analysis.

References

1. A. Lai *et al.*, *Eur. Phys. J.* C **22** 231 (2001).
2. J. R. Batley *et al.*, *Phys. Lett.* B **576**, 43 (2003).
3. G. D'Ambrosio, G. Ecker, G. Isidori and J. Portoles, JHEP **9808** 004 (1998).
4. M. Battaglia *et al.*, "The CKM matrix and the unitarity triangle", hep-ph/0304132
5. The KTeV Collaboration, *Phys. Rev.* D **64**, 112004 (2001).
6. E. Barberio and Z. Was, Comput. Phys. Commun. **79**, 291 (1994).
7. H. Fearing *et al.*, *Phys. Rev. Lett.* **24**, 189 (1970).
8. H. Fearing *et al.*, *Phys. Rev.* D **2**, 52 (1970).
9. M. G. Doncel, *Phys. Lett.* B **32**, 623 (1970).
10. B. R. Holstein, *Phys. Rev.* D **41**, 2829 (1990).
11. J. Bijnens *et al.*, *Nucl. Phys.* B **369**, 81 (1993).
12. G. Colangelo, J. Gasser, and H. Leutwyler, *Phys. Rev. Lett.* **86**, 5008 (2001).
13. G. Amoros, J. Bijnens and P. Talavera, *Nucl. Phys.* B **585**, 293 (2000).
14. A. Lai *et al.*, *Phys. Lett.* B **584**, 251 (2004).